Nov 7th, 12:00 AM - Nov 8th, 12:00 AM

Finite Element Modeling and Validation of Steel Sheathed Cold-Formed Steel Framed Shear Walls

Amanpreet Singh

Tara C. Hutchinson

Wei-Wen Yu International Specialty Conference on Cold-Formed Steel Structures
St. Louis, Missouri, U.S.A., November 7 & 8, 2018

Finite Element Modeling and Validation of Steel Sheathed Cold-formed Steel Framed Shear Walls

Amanpreet Singh[1], Tara C. Hutchinson[2]

Abstract

The objective of this paper is to validate the concept of utilizing a truss-element based finite element model for capturing the in-plane cyclic response of steel sheathed cold-formed steel (CFS) framed shear wall. The model is developed within the OpenSees finite element platform. Steel sheathed CFS shear walls show shear buckling of their sheathing as a tension field develops. This inelastic behavior of the shear walls is replicated by using the Pinching4 material for truss elements acting along the tension field. Importantly, the model employs beam-column elements for framing members, rotational springs for representing frame stiffness and vertical springs for modelling hold-downs. The wall models were calibrated using experimental data available for 0.030-in. and 0.033-in. steel sheet sheathed shear walls with 2:1 and 4:1 aspect ratios and 6-in., 4-in. and 2-in. fastener spacing at panel edges. The specimens were subjected to symmetric reverse cyclic displacement-controlled loading using the CUREE protocol. Comparison amongst the experimental and numerical models demonstrate a high degree of accuracy in the estimated shear strength and hysteretic response of the shear walls and as such has the potential to be an important building block towards modeling full structural systems constructed of cold-formed steel framing.

Introduction

The need for low-cost, multi-hazard resilient, mid-rise buildings makes Cold-Formed Steel (CFS) a popular choice for construction material offering many benefits such as lightweight framing, high durability and ductility, low installation and maintenance costs. Buildings framed with closely-spaced CFS members repetitively placed in the walls develop lateral resistance through sheathing attached to these members. CFS shear walls typically use wood panels or steel sheets as sheathing on one or both sides of the wall. The in-plane response of both of these systems has been explored extensively using component level experiments (eg. Serrette 2010, Liu et al. 2012, Yu 2010 and Shamin et al. 2013). Results from these and other experimental campaigns have been incorporated in

[1] Ph.D. Student, Department of Structural Engineering, University of California, San Diego, La Jolla, CA (ams082@eng.ucsd.edu)
[2] Professor, Department of Structural Engineering, University of California, San Diego, La Jolla, CA (tara@ucsd.edu)

structural design codes such as North American specifications AISI-S240 (2015) and AISI-S400 (2015). These experimental programs have been followed up by research on developing computational models that capture the non-linear behavior of CFS shear walls. For example, Buonopane et al. (2014) presents a fastener-based model for OSB sheathed shear walls in which every fastener is modeled by a non-linear, radially-symmetric zero length spring element. The fastener elements are assigned a material model which includes a softening backbone curve, pinching, and loading and unloading parameters. Kechidi et al. (2016) developed a new material model called CFSWSWP uniaxialMaterial implemented in OpenSees, which can simulate the deteriorating behavior, strength and stiffness degradation and pinched hysteretic response of wood-sheathed cold-formed steel shear walls. To contribute to the growing body of numerical modeling approaches for investigating the response of such systems, the present study evaluates an efficient truss-element based model for steel sheathed CFS shear wall system.

Experimental Program used for Numerical Validation

Fifteen sets each of monotonic and cyclic tests with two nominally identical shear walls were conducted to obtain shear strengths for wind loads and seismic loads (Yu et al. 2007). From these, nine sets of wall configurations tested cyclically were modeled, based on full-scale specimen details (Table 1, Figure 1). Complete details of the design and construction of the specimens can be obtained from Yu et al. (2007); however, it is noted that the same notation for the wall specimens adopted in the experiments have been used herein for consistency. The specimens were subjected to lateral cyclic displacement history following the CUREE protocol (Krawinkler et al. 2000) with no imposed vertical gravity load. The test walls modeled include two aspect ratios: 2:1 (4 ft. × 8 ft.) and 4:1 (2 ft. × 8 ft.), two sheet steel thicknesses: 0.033-in. and 0.030-in., and three fastener spacing on panel edges: 6-in., 4-in., and 2-in. The framing members (*350S162-43* for studs and *350T150-43* for tracks, ASTM A1003 Grade 33 steel) were assembled using #8 modified truss head self-drilling screws. Back to back double C-shaped structural studs were used for chord studs with the webs of these studs stitched together using 2-#8 self-drilling screws spaced at 6 in. o.c. Commercially available hold downs at each chord stud were used. Two 1/2-in. diameter Grade 8 were used for each wall. Sheathing was installed on one side using #8 self-drilling screws. Complete details of the experimental program can be found in Yu et al. (2007).

Table 1: Test matrix of shear walls modeled (test program of Yu et al. 2007)

Wall Set	Test Label	Wall dimensions (width × height × framing member thickness)	Steel sheet thickness	Fastener spacing, Perimeter/ Field
1	4×8×43×33-6/12-C1/C2	4 ft. × 8 ft. × 43 mil	33 mil	6 in./12 in.
2	4×8×43×33-4/12-C1/C2	4 ft. × 8 ft. × 43 mil	33 mil	4 in./12 in.
3	4×8×43×33-2/12-C1/C2	4 ft. × 8 ft. × 43 mil	33 mil	2 in./12 in.
4	4×8×43×30-6/12-C1/C2	4 ft. × 8 ft. × 43 mil	33 mil	6 in./12 in.
5	4×8×43×30-4/12-C1/C2	4 ft. × 8 ft. × 43 mil	33 mil	4 in./12 in.
6	4×8×43×30-2/12-C1/C2	4 ft. × 8 ft. × 43 mil	33 mil	2 in./12 in.
7	2×8×43×33-6/12-C1/C2	2 ft. × 8 ft. × 43 mil	33 mil	6 in./12 in.
8	2×8×43×33-4/12-C1/C2	2 ft. × 8 ft. × 43 mil	33 mil	4 in./12 in.
9	2×8×43×33-2/12-C1/C2	2 ft. × 8 ft. × 43 mil	33 mil	2 in./12 in.

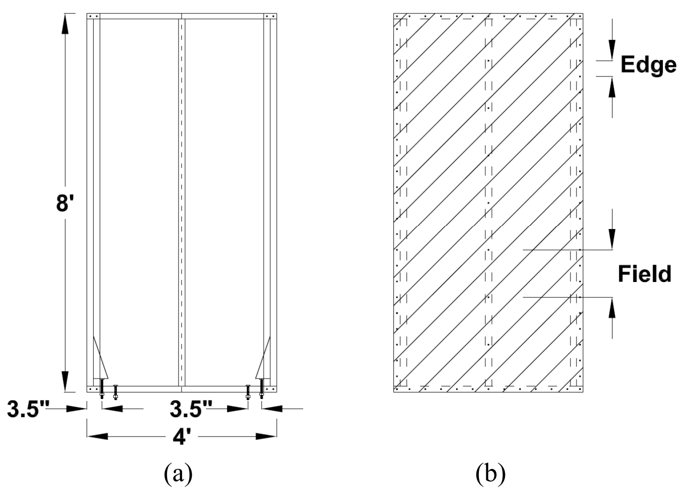

Figure 1: (a) Dimensions of 4 ft. × 8 ft. wall assembly, (b) Typical screw panel edge and field location schedule (See Table 1)

Description of Numerical Model

A schematic of the numerical model developed in OpenSees (McKenna et al. 2000) for capturing the in-plane cyclic response of the aforementioned shear wall specimens is provided in Figure 2. The CFS frame members, studs and tracks, are modeled using linear elastic, displacement beam-column elements. Chord studs use the full composite section properties for back to back structural studs. The studs and top/bottom tracks are connected using a rotational spring zero-length element to simulate a semi-rigid connection. The rotational stiffness of the spring is defined as 100 kip-in./rad [11.3 kN-m/rad], based on approximations from the measured lateral stiffness of bare CFS frame tests (Buonopane et al. 2014). Steel sheathed shear walls show significant pinching of their hysteretic lateral resistance with early onset of shear buckling in the sheathing, followed by development of a tension field, and finally by loss in lateral resistance and stiffness with damage at screw connections. The sheathing and connections are modeled as truss elements assigned with a Pinching4 material (Lowes et al. 2003), defined by a multi-linear backbone curve, stiffness and strength degradation, unloading and reloading parameters (Figure 3). In the present work, the cross-sectional area of the truss elements is assumed to be ten times the steel sheet thickness to approximately represent the width of the tension field. Due to the very large fastener spacing used for connecting the steel sheathing with the field studs, the interaction between the steel sheathing (truss elements) and field studs (beam-column element) is ignored in the numerical model. This had the added benefit of allowing the orientation of the truss elements to be along the tension field. The hold-downs are modeled as uniaxial vertical spring having an elastic stiffness of 99.3 kips/in [17.4 kN/mm] in tension, calculated based on published values of tensile strength and displacement (Simpson, 2017). In compression, the hold downs are bearing against a rigid foundation and thus the compressive stiffness is taken as 1000 times that of the tension stiffness (Leng et al. 2013). The horizontal DOF is restrained at locations of shear anchors and hold-downs.

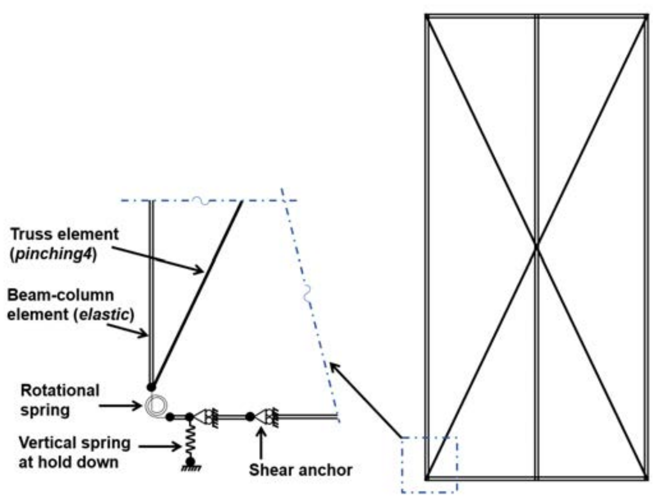

Figure 2: Numerical model of shear walls in OpenSees (shown for the 4 ft long walls)

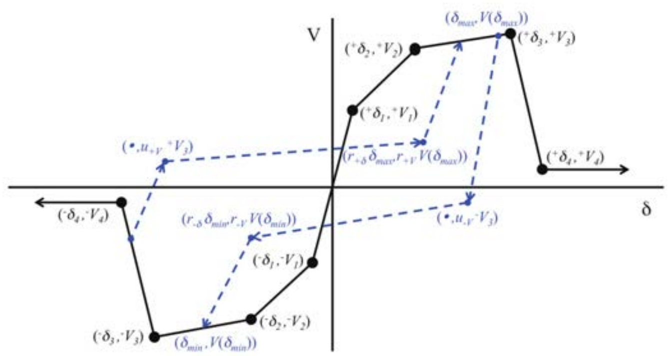

Figure 3: Pinching4 uniaxial material model (recreated from Lowes et al. 2003)

Results and discussion

The Pinching4 material requires definition of 39 parameters (Figure 3). To guide the definition of these parameters, the backbone for lateral resistance versus lateral displacement hysteretic response for each wall set was used to define the Pinching4 backbone. The material can be assigned two different backbone curves in the positive and negative excursions. However, since the hysteretic response of the tested walls was nearly symmetric, a symmetric backbone curve was assumed in the numerical representation. Similarly, unloading and reloading parameters were calibrated by systematically changing the parameters until a good fit between experimental and numerical model was obtained. The strength and stiffness degradation parameters of Shamin et al. (2013) were adopted. Table 2 lists the Pinching4 reloading, unloading and degradation parameters which were maintained for all sets of walls modeled. Table 3 lists the calibrated Pinching4 backbone curve parameters for all modeled walls. Figure 4, as an example, shows the comparison of the hysteretic response of the tested walls to that obtained using the best fit numerical model for wall set two.

Table 2: Pinching4 reloading, unloading and degradation parameters

$r_{+\delta}$	0.01	gK_1	0.5	gD_1	0.2	gF_1	0.0
$r_{-\delta}$	0.01	gK_2	0.5	gD_2	0.2	gF_2	0.0
r_{+V}	0.1	gK_3	1.5	gD_3	1.5	gF_3	0.0
r_{-V}	0.1	gK_4	1.5	gD_4	1.5	gF_4	0.0
u_{+V}	-0.2	gK_{lim}	0.8	gD_{lim}	0.25	gF_{lim}	0.0
u_{-V}	-0.2	gE	10.0		Damage type		Energy

Table 3: Calibrated Pinching4 parameters for positive branch (note that symmetric behavior is assumed, thus these also apply for negative branch)

Wall Set	$^+V_1$ kN	$^+V_2$ kN	$^+V_3$ kN	$^+V_4$ kN	$^+\delta_1$ ($\times 10^{-3}$) mm	$^+\delta_2$ ($\times 10^{-2}$) mm	$^+\delta_3$ ($\times 10^{-2}$) mm	$^+\delta_4$ ($\times 10^{-2}$) mm
1	27.3	56.5	71.0	21.6	6.9	3.3	9.1	18.2
2	38.5	61.0	77.3	32.1	7.5	3.5	9.0	19.8
3	59.2	79.2	88.3	40.2	1.5	0.20	8.4	20.0
4	18.5	43.0	55.5	19.0	11.0	6.0	14.1	28.0
5	25.5	50.8	64.9	26.0	14.0	5.5	13.2	30.0
6	33.0	58.5	69.0	31.0	17.0	5.0	10.1	31.0
7	23.5	57.0	69.9	22.0	0.40	2.8	8.8	22.0
8	31.0	55.0	79.9	26.0	0.65	2.0	6.4	24.0
9	33.0	50.0	89.1	26.0	1.0	1.5	5.6	24.0

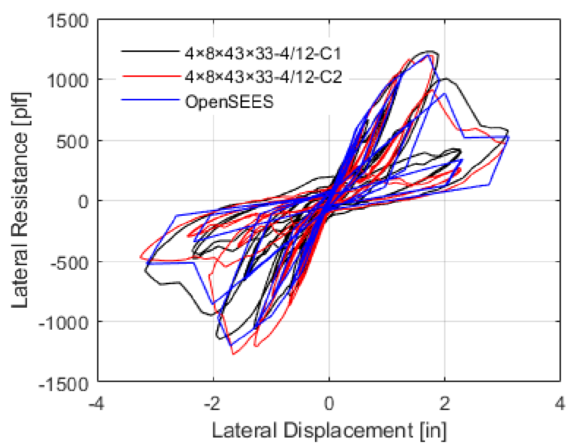

Figure 4: Comparison of experimental and numerical hysteretic response for wall set 2. (Specimens C1 and C2 are nominally identical)

Figures 5-7 show a comparison of experimental and numerical backbone curves and energy dissipated versus cumulative displacement for all wall sets modeled. These comparisons demonstrate the capability of the simple X-brace type numerical models proposed herein. Importantly, the OpenSees models are able to capture the highly pinched lateral resistance versus displacement hysteretic behavior and energy dissipation through formation of the tension field as the cycle amplitude increases and the behavior becomes highly non-linear. For walls with 4:1 aspect ratio, energy dissipation is not correctly captured after cycle with peak strength, with error as high as 45% at the end of displacement history.

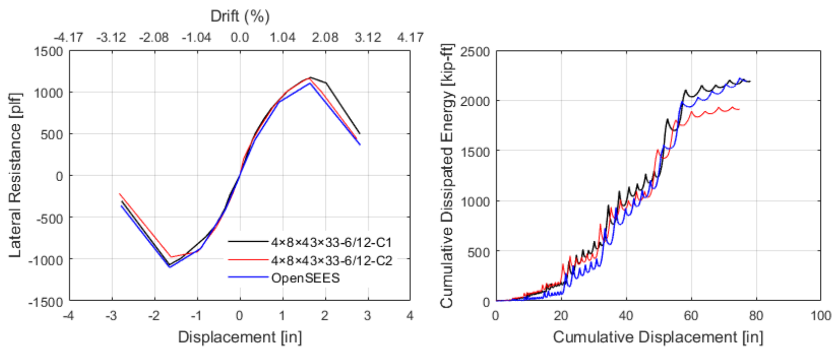

(a) Wall set 1

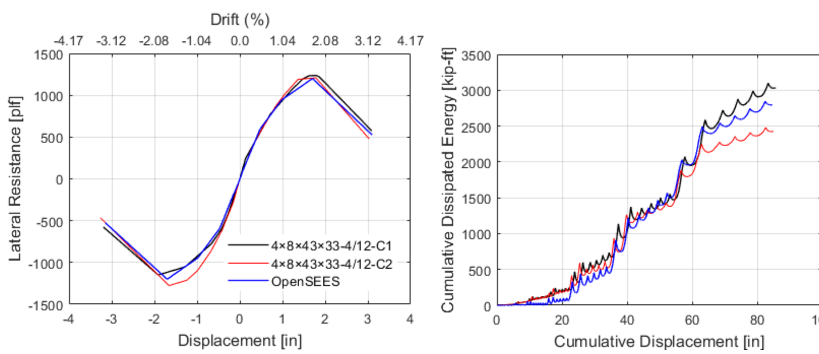

(b) Wall set 2

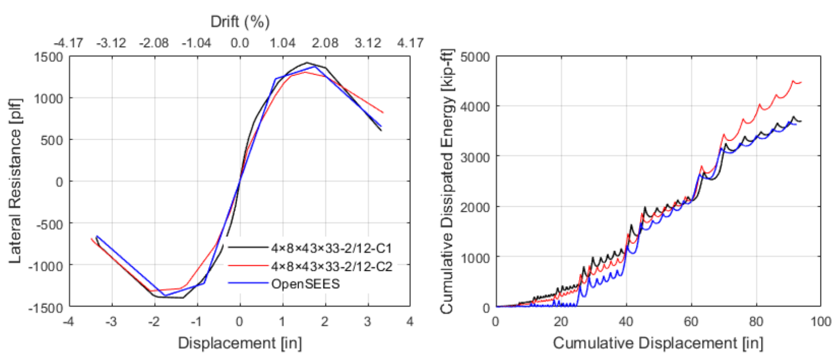

(c) Wall set 3

Figure 5: Comparison of experimental and numerical backbone curves and cumulative dissipated energy for wall sets 1-3

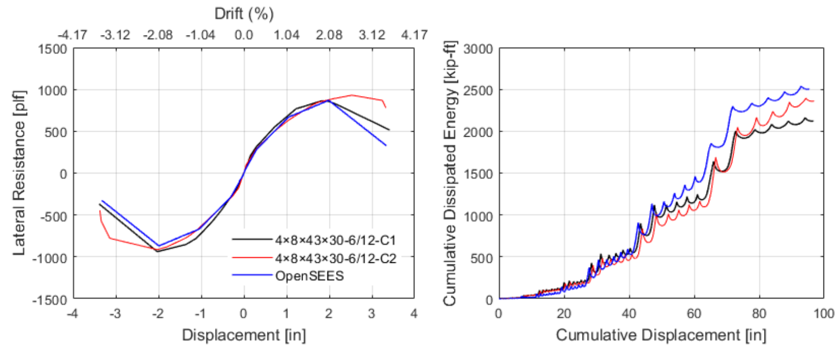

(a) Wall set 4

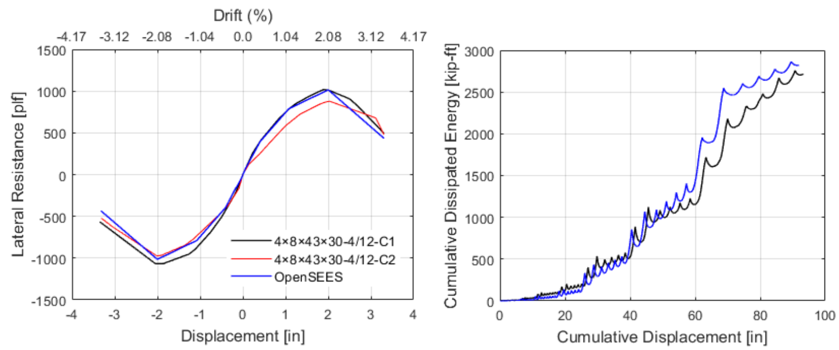

(b) Wall set 5

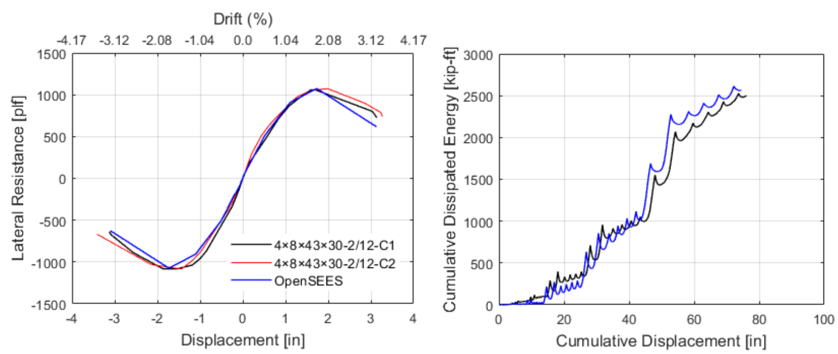

(c) Wall set 6

Figure 6: Comparison of experimental and numerical backbone curves and cumulative dissipated energy for wall sets 4-6

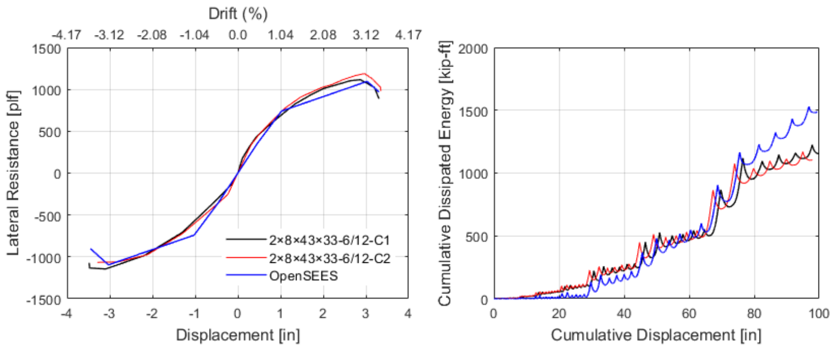

(a) Wall set 7

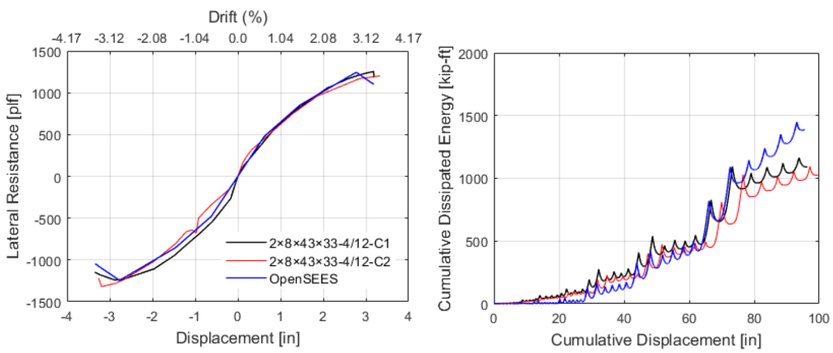

(b) Wall set 8

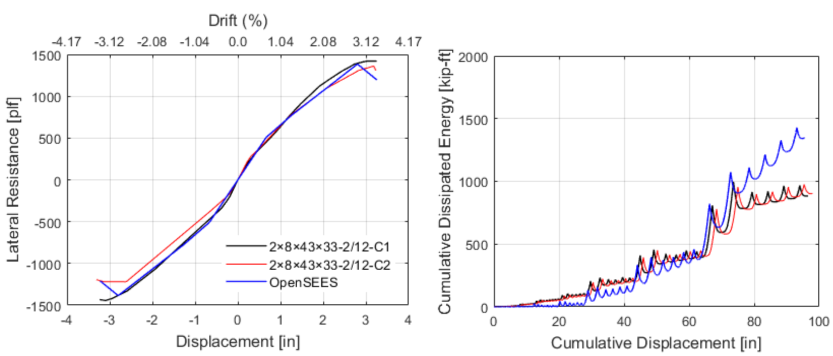

(c) Wall set 9

Figure 7: Comparison of experimental and numerical backbone curves and cumulative dissipated energy for wall sets 7-9

This modeling strategy can be extended to include other steel sheet thicknesses and framing member sizes by calibrating against additional experimental datasets. This shear wall model can also be used as a building block for models intended to capture the coupled shear wall and gravity wall behavior and exploring the contribution of gravity walls to the overall lateral resistance. In this study, the framing members are modeled as linear elastic members. However, if the intent was to capture framing member behavior and other sources of non-linearity and energy dissipation, inelastic beam-column elements would be needed to model studs and tracks.

Conclusions

A series of wall configurations tested cyclically by Yu et al. (2007) were modeled using an efficient, and low degree-of-freedom truss-element based finite element model in OpenSees. The parameters of the selected nonlinear Pinching4 material model were calibrated to obtain a best fit to the experimental response. The models were able to capture the severely pinched hysteretic response and energy dissipated through displacement cycles. The study shows the capability of X-brace type numerical models to capture steel sheathed shear wall behavior and a set of calibrated Pinching4 parameters for nine sets of walls considered are provided.

Acknowledgments

The first author was partially funded through the National Science Foundation (NSF) grant CMMI 1663569, project entitled: *Collaborative Research: Seismic Resiliency of Repetitively Framed Mid-Rise Cold-Formed Steel Buildings*. Collaborative discussions of project partners Professors Ben Schafer and Kara Peterman, as well as students engaged in this collaborative effort at Johns Hopkins and University of Massachusetts-Amherst, are greatly appreciated. The opinions and findings expressed in this paper are those of the authors and do not necessarily reflect the views of the funding agencies.

References

AISI-S240-15 (2015). "North American Standard for Cold-Formed Steel Structural Framing." *American Iron and Steel Institute: Washington, D.C.*

AISI-S400-15 (2015). "North American Standard for Seismic Design of Cold-Formed Steel Structural Systems." *American Iron and Steel Institute: Washington, D.C.*

Buonopane, S. G., Tun, T. H., and Schafer, B. W. (2014). "Fastener-based computational models for prediction of seismic behavior of CFS shear walls."

In *Proceedings of the 10th National Conference in Earthquake Engineering*. EERI Anchorage, AK.

Kechidi, S., and Bourahla, N. (2016). "Deteriorating hysteresis model for cold-formed steel shear wall panel based on its physical and mechanical characteristics." *Thin-Walled Structures, 98*, 421-430.

Krawinkler, H., Parisi, F., Ibarra, L., Ayoub, A. and Medina, R. (2000). "Development of a testing protocol for woodframe structures." Consortium of Universities for Research in Earthquake Engineering (CUREE) Publication No. W-02, Richmond, CA:

Leng, J., Schafer, B. W., and Buonopane, S. G. (2013). "Modeling the seismic response of cold-formed steel framed buildings: model development for the CFS-NEES building." In *Proceedings of the Annual Stability Conference-Structural Stability Research Council*, St. Louis, Missouri.

Liu, P., Peterman, K. D., Yu, C., and Schafer, B. W. (2012). "Characterization of Cold-formed Steel Shear Wall Behavior under Cyclic Loading for the CFS-NEES Building." In *Proceedings of 21th International Specialty Conference on Cold-Formed Steel Structures*, St. Louis, Missouri.

Lowes, L. N., Mitra, N., and Altoontash, A. (2003). "A beam-column joint model for simulating the earthquake response of reinforced concrete frames." PEER Rep. 2003/10.

McKenna F., Fenves G. L., Scott M. H. and Jeremic B. (2000). Open System for Earthquake Engineering Simulation (OpenSees). Pacific Earthquake Engineering Research Center, University of California, Berkeley, CA.

Serrette, R. (2010). "Seismic Design Strength of Cold-Formed Steel-Framed Shear Walls." ASCE *Journal of Structural Engineering* 136 (9): 1123–1130.

Shamim, I., DaBreo, J., and Rogers, C. A. (2013). "Dynamic testing of single-and double-story steel-sheathed cold-formed steel-framed shear walls." ASCE *Journal of Structural Engineering, 139*(5), 807-817.

Shamim, I., and Rogers, C. A. (2013). "Steel sheathed/CFS framed shear walls under dynamic loading: numerical modelling and calibration." *Thin-Walled Structures, 71*, 57-71.

Simpson Strong-Tie Company Inc. (2017). "S/HDS and S/HDB Holdowns." Simpson Strong-Tie Company Inc.

Yu, C., Vora, H., Dainard, T., and Veetvkuri, P. (2007). "Steel sheet sheathing options for CFS framed shear wall assemblies providing shear resistance." Denton, USA: Department of Engineering Technology, University of North Texas (Report No. UNT-G76234).

Yu, C. (2010). "Shear resistance of cold-formed steel framed shear walls with 0.686 mm, 0.762 mm, and 0.838 mm steel sheet sheathing." *Engineering Structures, 32*(6), 1522-1529.